

Negative Incremental Resistance Induced by Calcium in Asymmetric Nanopores

Zuzanna S. Siwy,^{*,†} Matthew R. Powell,[†] Eric Kalman,[†] R. Dean Astumian,[‡] and Robert S. Eisenberg[§]

University of California, Irvine, Department of Physics and Astronomy, Irvine, California 92697, University of Maine, Department of Physics, Orono, Maine 04469, and Rush Medical College, Department of Molecular Biophysics & Physiology, Chicago, Illinois 60612

Received December 8, 2005; Revised Manuscript Received January 23, 2006

ABSTRACT

Single polymer nanopores with permanent surface charges act as rectifiers of ionic current. The pores are tapered cones with narrow openings of several nanometers and wide openings of $\sim 1 \mu\text{m}$. The pores are cation-selective, and in symmetric solutions of potassium chloride they rectify the flow of potassium ions from the small opening toward the wide opening. Millimolar concentrations of calcium reverse the rectification, and a negative incremental resistance is observed. These observations can be interpreted by a model containing flashing ratchets.

Introduction. Nanopores have been investigated widely because of their importance in nanotechnology and their crucial role as biological channels that control many physiological processes.^{1–3} The transport properties of these systems are usually studied as the ion current passing through a single channel as a function of time, voltage, and type and concentration of ions. Nanopores have new transport properties not observed in larger micropores, their micrometer-scale counterparts.⁴ Rectification of ion current observed in nanoscale pores is usually seen as asymmetric, diode-like current–voltage (I – V) curves.^{5,6} Nanopores rectify ion current if they are asymmetric, for example, if they are shaped as tapered cones and have permanent surface charges on the walls of the pore.^{4,7,8} These rectifying tapered conical pores were prepared by a track-etching technique that starts by irradiating a polymer film with energetic heavy ions. The latent tracks left by the heavy ions^{5–7,9} are then etched chemically in an asymmetric way. The walls of these pores are covered with carboxylate groups that form the permanent negative charge on the pore walls^{5,6} (at neutral and basic pH).

The rectifying properties of these pores have been studied using potassium chloride as the electrolyte that carries current through the channel in a simple robust apparatus that has parasitic shunt impedances $> 10^{11} \Omega$.^{5,7} Because lipid bilayers are not involved, the apparatus is fundamentally

rugged in a way not yet achieved in bilayer or patch pipet setups. The effect of ion current rectification has been modeled by looking at electrostatic interactions of potassium and chloride ions with the surface charges on the pore walls.^{5,7,8} The effective electric field that exerts a force on ions passing through the nanopore has been treated as a sum of internal electric field produced by the permanent charge on the pore walls and the externally applied potential difference, assuming that the internal and external fields do not alter the underlying charge distributions.

In this letter we describe a conical nanopore system bathed in mixtures of ~ 100 mM potassium chloride and micromolar to millimolar calcium chloride. As discussed below, we presume that the profile of internal electric potential of a nanopore is changed by the calcium ions. We think that these calcium ions interact in a time-dependent way with the permanent charge of the pore, producing a time varying potential field inside the channel that influences the net ion current through it. We propose that fluctuations in the total charge inside the channel, that is, the charge of mobile ions, permanent charge, and dielectric boundary charge, produce fluctuating potentials and negative incremental resistance that reverses the direction of rectification. A quantitative model is surely needed to make this proposal precise, but we think that the qualitative phenomena and experimental evidence are so striking that they should be reported immediately: the construction of even a low-resolution (time-dependent Poisson–Nernst–Planck (PNP)) type model of such fluctuations will not be easy and will not be convincing until it is

* Corresponding author. E-mail: zsiwy@uci.edu.

[†] University of California, Irvine.

[‡] University of Maine.

[§] Rush Medical College.

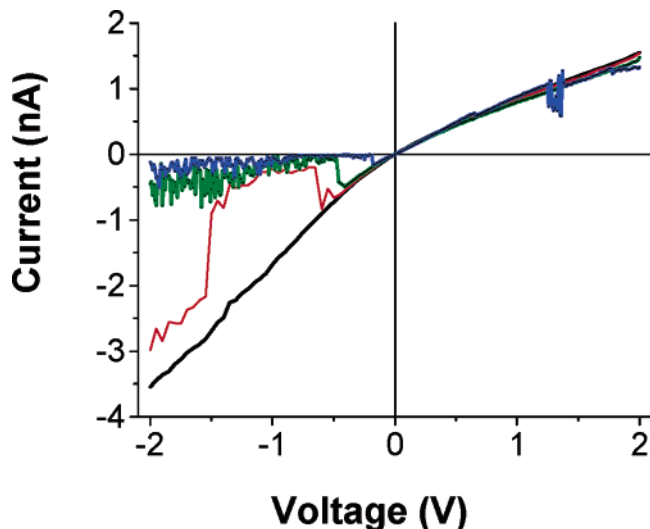


Figure 1. Current–voltage curves recorded for a single PET nanopore at symmetric electrolyte conditions and pH 8: black curve, 0.1 M KCl; red curve, 0.1 M KCl + 0.1 mM CaCl₂; green curve, 0.1 M KCl + 0.4 mM CaCl₂; blue curve, 0.1 M KCl + 0.7 mM CaCl₂. The voltage sweep was in the direction from +2 V to –2 V with 50 mV steps. Voltage is defined as $V_b - V_t$. The diameters of the conical nanopore are $d_t = 5$ nm and $d_b = 890$ nm.

derived from a high-resolution theory with atomic detail in appropriate places. No one knows how to construct or compute a calibrated high-resolution model including atomic length scales of the pore (Å) and the macroscopic time scales of our experiment (milliseconds).

Experimental Results. The nanopores presented in this letter were prepared in 12- μ m-thick poly(ethylene terephthalate) (PET) (Hostaphan RN12, Hoechst) by single heavy ion irradiation and subsequent asymmetric chemical etching of the tracks.^{5–7,10} This procedure leads to the formation of tapered-cone nanopores with two openings, one with a diameter in the micrometer range and the other with a diameter as small as ~ 2 nm.¹¹ The wide opening of the pore will be called the base (with diameter d_b); the narrow opening of the pore will be called the tip (with diameter d_t).

Figure 1 (black curve) shows the rectifying current–voltage characteristic of a single PET nanopore recorded in identical (i.e., “symmetric”) electrolyte solutions of 0.1 M KCl, pH 8. The pore diameters are $d_t = 5$ nm and $d_b = 890$ nm. The diameters were measured as described in refs 6 and 10. The grounded electrode was on the tip side. The potential differences are computed as $V_b - V_t$ where V_b and V_t are potentials of the electrodes on the base and tip side, respectively. Ohm’s law is then written as $i = g(V_b - V_t)$ with $g \geq 0$, and thus positive i means that cations flow from base to tip. As has been shown previously, PET nanopores at neutral and basic pH are cation-selective.^{7,11} The cations flow with less resistance from the tip toward the base than from base to tip.

The I – V curves change dramatically when we add calcium ions at millimolar concentration to both sides of the membrane (Figure 1). We used the chloride salt of calcium CaCl₂ to avoid introducing additional anions to the system and made no attempt to buffer Ca²⁺ concentrations. The pH

of the salt solutions was adjusted to values of 7.8–8.0 with ~ 2 mM phosphate buffer, thereby ionizing carboxylates and keeping the surface charge of the walls of the pore negative.¹² (We assume that the net permanent charge of the pore walls is not influenced by mutual electric and steric interactions of neighboring carboxylate groups or the dielectric constant of the polymer matrix and so forth.¹³)

Two effects were observed with calcium present in the system. At negative $V_b - V_t$, larger magnitudes (we define “magnitude” by the absolute value function, e.g., $|V_b - V_t|$) of voltage resulted in smaller magnitudes of ion current, an effect called negative incremental resistance. Additionally, with calcium in the system, the direction of rectification reversed compared to rectification when only KCl was present (at 0.1 M concentration: black curve, Figure 1). Figure 1 shows how the I – V curve changes when the concentration of calcium is changed. At higher calcium concentrations, the negative incremental resistance occurred at smaller magnitudes of $V_b - V_t$. There is a clear threshold for negative $V_b - V_t$ at which the negative incremental resistance starts to occur: with 0.1 mM CaCl₂ it started at -0.65 V, with 0.4 mM CaCl₂ at -0.45 V and with 0.7 mM CaCl₂ at -0.20 V. It is important to note that the effect of negative incremental resistance was reproducible at 0.4 and 0.7 mM CaCl₂ but not at 0.1 mM. At 0.1 mM CaCl₂ the effect did not occur in every voltage sweep, suggesting that the concentration of calcium was not high enough to maintain the same value in each sweep. We imagine that the concentration fluctuated too strongly to support the negative incremental resistance in every sweep.

Higher calcium concentration also led to smaller magnitudes of ion current in the cation direction from tip to base (in our electrode configuration at negative $V_b - V_t$).

As mentioned above, with the presence of calcium, we see rectification in the opposite direction to that observed with only KCl. We wanted to check whether the rectification effect can support net ionic transport against the electrochemical gradient, an effect observed before with KCl in the direction from tip to base.^{5,7} We kept the calcium concentration the same on both sides of the membrane and applied a KCl concentration gradient with higher KCl concentration on the tip side. In this case the potassium ions would be transported against the concentration gradient from base to tip. Figure 2 shows an I – V curve recorded at 0.15 M KCl with 0.7 mM CaCl₂ on the tip side and 0.1 M KCl with 0.7 mM CaCl₂ on the base side. The rectification direction is still preserved with higher currents for positive $V_b - V_t$ than currents for negative $V_b - V_t$. If we average the ion current along the whole voltage sweep from -2 V to $+2$ V, then we get a positive value of net current 0.149 ± 0.042 nA (average over four voltage sweeps) that provides evidence for ionic transport against the electrochemical gradient, from base to tip.

We also investigated the influence of permanent surface charge on the occurrence of the negative incremental resistance and the effect of reversing the direction of rectification. Figure 3 shows I – V curves for a single conical nanopore recorded at symmetric electrolyte conditions of 0.1

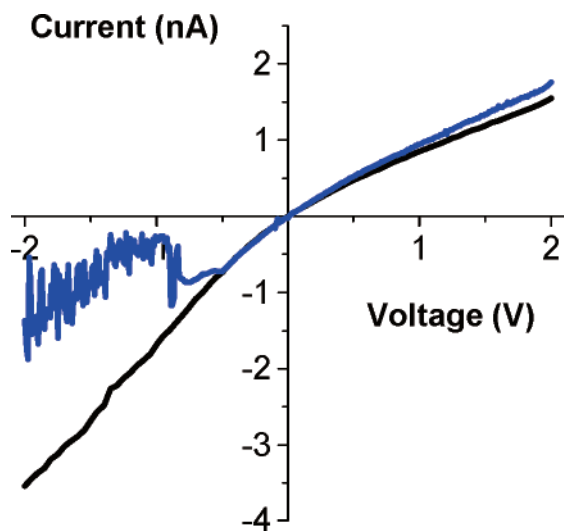


Figure 2. Current–voltage curve for a single PET pore (the same as in Figure 1) recorded at 0.1 M KCl + 0.7 mM CaCl₂ on the base side and 0.15 M KCl + 0.7 mM CaCl₂ on the tip side (blue curve). For comparison, the I – V curve recorded at symmetric conditions of 0.1 M KCl and pH 8 is shown as well (black curve). Voltage is defined as $V_b - V_t$. Close examination of the blue curve around $V_b - V_t = 0$ shows that there is a finite current of ca. –20 pA, as expected with the KCl concentration gradient.

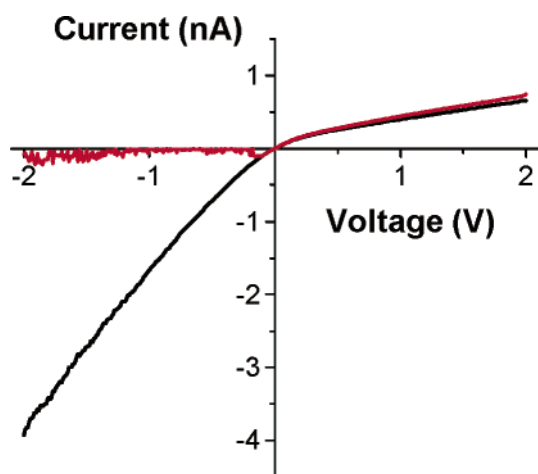


Figure 3. Current–voltage curve of a single conical nanopore recorded at 0.1 M KCl and 1 mM CaCl₂ buffered to pH 6 (black curve) and pH 8 (red curve). Voltage is defined as $V_b - V_t$. The diameters of the conical nanopore are $d_t = 7$ nm and $d_b = 610$ nm.

M KCl with 1.0 mM CaCl₂ at pH 8 and pH 6, adjusted with phosphate buffer (~2 mM). At more acidic conditions, because of protonation of carboxylate groups of the pore walls, we expected to achieve a lower net surface charge¹². We have observed that lowering pH by two units changed the I – V curve back to the shape that is recorded at KCl solutions without calcium (Figure 3).

Interaction of Calcium Ions with Permanent Charges of Pore Walls. To understand the effect of calcium on the transport properties of conical nanopores, we first considered interactions of calcium ions with permanent surface charges on the pore walls. Adding even a millimolar concentration of divalent cations has a dramatic influence on the electric potential at the interface between solids and ionic solutions

because divalents screen surface charges strongly.^{14,15} In our case, we know this screening effect is reversible: after each set of measurements with one calcium concentration, we exchanged the electrolyte in the conductivity cell back to 0.1 M KCl at pH 8, which resulted in recording an I – V curve identical to the one shown in Figure 1 as a black curve.

An important issue to consider is how calcium ions interact with the surface on time scales comparable to the time that potassium ions take to move through the pore.

The surface of track-etched PET membrane and on the pore walls have 1.5 carboxyl (COO[–]) groups per square nanometer.¹⁵ One can expect therefore that the lumen of the conical pore resembles the so-called “selectivity filter” or locus of a biological calcium channel, and of the chemical ethylenediaminetetraacetic acid (EDTA), for that matter, where four carboxylate groups concentrated into a tiny volume have effective binding (formation) constants, K_{eff} , as high as 10^8 M^{-1} .^{16,17}

The effective binding or formation constant can be expressed as a ratio of rates of calcium binding to carboxylate groups and calcium unbinding, the so-called $k_{\text{on}} = t_{\text{on}}^{-1}$ and $k_{\text{off}} = t_{\text{off}}^{-1}$. The maximum value of t_{on}^{-1} is usually estimated as if reactants were uncharged, from the diffusion limit of a chemical reaction of an hypothetical uncharged calcium (implying that every calcium ion that enters the pore binds^{1,18}). Taking the diffusion coefficient for ions $D = 10^9 \text{ nm}^2/\text{s}$ and radius of the pore $r = 5$ nm one obtains $k_{\text{on}} \approx 10^9 \text{ (M}^{-1}\text{s}^{-1})$ for the hypothetical uncharged calcium binding to an uncharged binding site. The off rate could similarly be estimated as $k_{\text{on}}/K_{\text{eff}}$. Thus, calcium ions can stay bound to the carboxylate groups for times ~0.1 s. One can calculate similar quantities for ions using only their electrical properties and ignoring their diffusion. The ionic mobility of potassium ions is $\sim 10^{-8} \text{ V}/(\text{m}^2\cdot\text{s})$.¹⁹ If the electric field is 1 V over 12 micrometers, then the drift velocity of ions in solution reaches $\sim 10^{-3} \text{ m/s}$. The ions therefore translocate the pore within ~1 ms. Calcium ions can indeed stay at the charged surface for times comparable to the time that potassium ions need to translocate the pore. These calculations have been performed using bulk properties of electrolytes. As discussed, however, in ref 20 and other places, this approach allows at least a semiquantitative description of the transport properties of pores with diameters of several nanometers.

We present a possible explanation of the effect of negative incremental resistance observed with calcium by a ratchet model.

Flashing Ratchet Model for Ca-Induced Pumping and Apparent Reversal of Rectification Properties. Because of the physical asymmetry of the pore, the potential energy profile for an ion due to electric interactions with permanent surface charges is also asymmetric. The asymmetry has been modeled explicitly by two approaches: (i) through integrated electrostatic interactions between a cation inside the pore with negative charges on the pore walls at various positions inside the pore,^{5,7} and (ii) from PNP modeling.²¹ Convincing models are likely to need more atomic detail, but calibrated computation of an atomic detail model is a formidable

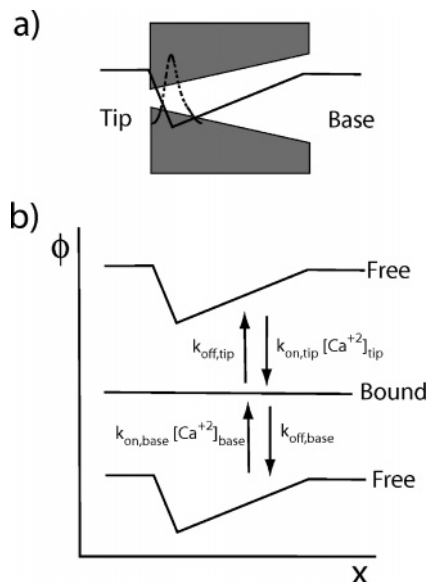


Figure 4. (a) Representation of the pore geometry on which the schematic piecewise linear potential profile for the case of negative surface charge on the interior of the pore is superposed. The dashed line illustrates the equilibrium concentration profile for potassium within the pore. (b) Schematic illustration of how the potential profile within the pore changes depending on whether calcium is specifically bound near the tip of the pore or not. The voltage dependence of the on and off rates for Ca binding through the narrow access tip ($k_{\text{on,tip}}$, $k_{\text{off,tip}}$ in Figure 4b) is greater than the voltage dependence of the on and off rates through the less resistive base ($k_{\text{on,base}}$, $k_{\text{off,base}}$). The concentrations $[\text{Ca}]_{\text{tip}}$ and $[\text{Ca}]_{\text{base}}$ refer to the local concentration at the mouth of the tip and base, respectively.

challenge, particularly on the millisecond time scale of experimental data.

In Figure 4a and b we see a simple heuristic depiction of the potential as a piecewise linear well resembling an asymmetric sawtooth. Because of the asymmetry, the mobility (conductance) is an asymmetric function of the electrochemical potential gradient,²² that is, the pore behaves as a rectifier. This is how we have explained rectification of our pores at $\text{KCl}^{5,7,8,23-26}$ (black curve in Figure 1). What about the effect of calcium and negative incremental resistance?

Here we propose a model in which calcium binding dramatically decreases the depth of the potential well shown in Figure 4a. At steady state without calcium, there is a population of ions, in our case potassium ions, in the well at any time, most of which are near the bottom of the well and hence near the left-hand reservoir (dashed curve in Figure 4a). This distribution of potassium ions of course fluctuates because of thermal noise. Sometimes the peak is to the left of the minimum, but more often (because of the gentler slope) the peak of the distribution is to the right of the minimum of the potential.

In Figure 4b we give a schematic picture of how the transport of calcium through the channel down its electrochemical gradient can induce pumping of potassium according to the flashing ratchet mechanism.^{28,29} When the voltage drives calcium from the tip to the base, the sequence of events can be sketched out; Ca enters the pore through the tip and binds to carboxylate groups near the bottom of the

potential well. One or a few calciums dramatically decrease the depth of the well.²⁷ In the case when Ca is bound, we model the potential as being flat, for simplicity. The potassium ions in the well begin to diffuse with equal probability to the left and to the right. Because the center of their distribution is much closer to the tip, many more ions exit through the tip than through the base. After some Poisson distributed time, the calcium ion dissociates, returning the potential to the deep well shape (Figure 4a). Now potassium ions must repopulate and will do so by moving through the base of the nanopore, which is much wider than the tip (through which most ions exited). This scenario is repeated each time the calcium binds and releases. Because the potential fluctuates, flashing “on” and “off”, the mechanism is called a flashing ratchet.^{24,28,29} The exit of ions is predominantly through the tip and the entrance of ions is predominantly through the base; therefore, this Ca association/dissociation leads naturally to net pumping of ions from base to tip. This direction is against the electrochemical gradient of potassium (hence, we describe it as pumping) and works to cancel the background rectified current, resulting in the observed negative incremental resistance.

The direction of pumping is set by the asymmetry of the pore and is from base to tip. It is not necessary for the nonequilibrium fluctuations to have a well-defined single frequency, nor is any coherence needed. It is necessary, however, that the fluctuations be driven by an energy source (in our case an electrochemical potential difference of Ca across the membrane and an applied voltage) to overcome the symmetry imposed by the detailed balance that holds at equilibrium.²⁴ We distinguish on and off rates for Ca binding through the narrow access tip ($k_{\text{on,tip}}$, $k_{\text{off,tip}}$ in Figure 4b) and on and off rates through the less resistive base ($k_{\text{on,base}}$, $k_{\text{off,base}}$ in Figure 4b). The rate constants depend on the potential difference $V_b - V_t$ such that the overall equilibrium constant has a form

$$\frac{k_{\text{on,tip}}k_{\text{off,base}}}{k_{\text{on,base}}k_{\text{off,tip}}} = \exp[-2(V_b - V_t)/kT]$$

Because the voltage drop across the narrow tip of the nanopore is much greater than that across its wide base, the dependence of $k_{\text{on,tip}}$ and $k_{\text{off,tip}}$ on voltage is much stronger than the dependence of $k_{\text{on,base}}$ and $k_{\text{off,base}}$ on voltage. This weak voltage dependence of $k_{\text{on,base}}$ and $k_{\text{off,base}}$ explains why the pumping is much greater when the voltage drives Ca from the tip to the base than when the voltage drives Ca from the base to the tip.

In Figure 4b we marked the local concentrations of calcium at the mouth of the tip and base, as $[\text{Ca}]_{\text{tip}}$ and $[\text{Ca}]_{\text{base}}$, respectively. At equilibrium ($V_b - V_t = 0$ and bulk concentrations of calcium on the tip and base side equal) the local calcium concentrations fluctuate, as does the local concentration of potassium in the pore. These fluctuations are strongly correlated by electrostatic interactions, resulting in a symmetry condition known as detailed balance in which every process is exactly as likely as the reverse of that process. Thus, despite the physical asymmetry of the pore,

fluctuation (flashing) of the potential due to equilibrium association/dissociation of calcium does not lead to directed transport.²⁴

The situation is entirely different when calcium is driven through the pore by an external voltage. In this case the effect of the correlation between fluctuations of the calcium concentration and the potassium concentration is reduced or eliminated altogether. Detailed balance no longer holds, and the physical asymmetry now produces a net pumped current of potassium from the base to the tip side of the nanopore.

Pumping by a flashing ratchet mechanism further requires that the lifetime of calcium at the binding site is longer than the time potassium takes to leave the pore. As explained above, increasing $V_b - V_t$ decreases the lifetimes of calcium in the bound state. For small(ish) voltages, this effect leads to an increase of the pumped current because we have more events of flipping the potential profile as shown in Figure 4b. At very high voltages, however, and low calcium concentration, k_{on} and k_{off} become too big, so there is insufficient time for the channel to empty while Ca is bound. For 0.1 mM $CaCl_2$ and $V_b - V_t < -1.5$ V, the ion current (red curve in Figure 1) approaches values of ion current observed without calcium (black curve in Figure 1). At higher concentrations of calcium, we do not see larger currents for negative voltages. This might be because we have not studied the behavior of our pore at higher voltages.³⁰ Another explanation for such low ion currents at large magnitudes of negative $V_b - V_t$ includes a calcium-induced block of the pore.³¹

We have given a rough heuristic description of how a negative incremental resistance observed experimentally can arise from a flashing ratchet mechanism driven by the nonequilibrium transport of calcium. We will expand our model to incorporate greater detail in a subsequent paper.

Conclusions. We have presented a single asymmetric nanopore system whose rectifying properties are changed dramatically by addition of a millimolar concentration of calcium ions. We think that binding and unbinding of calcium ions to the pore walls produces ion pumping by a flashing ratchet mechanism, although other interpretations may also be possible. We expect that nanopores of smaller diameters will be sensitive to lower calcium concentrations. In our present experimental system with pore diameters $\sim 3-7$ nm, not every calcium ion that arrives at the pore entrance will bind to the pore. With smaller pores we expect to reach calcium sensitivity comparable to biological L-type calcium channels, with micromolar sensitivity.¹ We will also try to separate different ionic species.

Acknowledgment. Irradiation with swift heavy ions was performed at the Gesellschaft fuer Schwerionenforschung

(GSI), Darmstadt, Germany. We are very grateful for many discussions with Prof. Charles R. Martin. Research was supported by a grant from the NIH GM 067241 (R.S.E. Principal Investigator).

References

- (1) Hille, B. *Ionic Channels of Excitable Membranes*, 2nd ed.; Sinauer: Sunderland, MA, 1992.
- (2) Bayley, H.; Martin, C. R. *Chem. Rev.* **2000**, *100*, 2575–2594.
- (3) Ashcroft, F. M. *Ion Channels and Disease*; Academic Press: New York, 1999.
- (4) Siwy, Z. *Adv. Funct. Mater.*, in press.
- (5) Siwy, Z.; Fulinski, A. *Phys. Rev. Lett.* **2002**, *89*, 198103/1–198103/4.
- (6) Siwy, Z.; Apel, P.; Baur, D.; Dobrev, D.; Korchev, Y. E.; Neumann, R.; Spohr, R.; Trautmann, C.; Voss, K. *Surf. Sci.* **2003**, *532–535*, 1061–1066.
- (7) Siwy, Z.; Fulinski, A. *Am. J. Phys.* **2004**, *72*, 567–574.
- (8) Siwy, Z.; Heins, E.; Harrell, C. C.; Kohli, P.; Martin, C. R. *J. Am. Chem. Soc.* **2004**, *126*, 10850–10851.
- (9) Fleischer, R. L.; Price, P. B.; Walker, R. M. *Nuclear Tracks in Solids. Principles and Applications*; University of California Press: Berkeley, CA, 1975.
- (10) Apel, P. Y.; Korchev, Y. E.; Siwy, Z.; Spohr, R.; Yoshida, M. *Nucl. Instrum. Methods Phys. Res., Sect. B* **2001**, *184*, 337–346.
- (11) Siwy, Z.; Gu, Y.; Spohr, H. A.; Baur, D.; Wolf-Reber, A.; Spohr, R.; Apel, P.; Korchev, Y. E. *Europhys. Lett.* **2002**, *60*, 349–355.
- (12) Wolf, A.; Reber, N.; Apel, P. Y.; Fischer, B. E.; Spohr, R. *Nucl. Instrum. Methods Phys. Res., Sect. B* **1995**, *105*, 291–293.
- (13) Varma, S.; Jakobsson, E. *Biophys. J.* **2004**, *86*, 690–704.
- (14) Israelachvili, J. *Intermolecular and Surface Forces*, 2nd ed.; Academic Press: London, 1991.
- (15) Bashford, C. L.; Alder, G. M.; Pasternak, C. A. *Biophys. J.* **2002**, *82*, 2032–2040.
- (16) Nonner, W.; Catacuzzeno, L.; Eisenberg, B. *Biophys. J.* **2000**, *79*, 1976–1992.
- (17) NIST Standard Reference Database 46, <http://www.nist.gov/srd/nist46.htm>.
- (18) Almers, W.; McCleskey, E. W. *J. Physiol.* **1984**, *353*, 585–608.
- (19) Atkins, P.; de Paula, J. *Physical Chemistry*, 7th ed.; W. H. Freeman and Company: New York, 2002.
- (20) Fulinski, A.; Kosinska, I.; Siwy, Z. *Europhys. Lett.* **2004**, *67*, 683–689.
- (21) Cervera, J.; Schiedt, B.; Ramirez, P. *Europhys. Lett.* **2005**, *71*, 35–41.
- (22) Risken, H. *The Fokker-Planck Equation: Methods of Solution and Applications*; Springer-Verlag: Berlin, 1989.
- (23) Hanggi, P.; Bartussek, R. In *Nonlinear Physics of Complex Systems*; Parisi, J., Mueller, S. C., Zimmermann, W., Eds.; Springer: Berlin, 1996, *476*, 294–308.
- (24) Astumian, R. D. *Science* **1997**, *276*, 917–922.
- (25) Reimann, P. *Phys. Rep.* **2002**, *361*, 57–265.
- (26) Magnasco, M. O. *Phys. Rev. Lett.* **1993**, *71*, 1477–1481.
- (27) (a) Dang, T. X.; McCleskey, E. W. *J. Gen. Physiol.* **1998**, *111*, 185–193. (b) McCleskey, E. W. *J. Gen. Physiol.* **1999**, *113*, 765–772.
- (28) Astumian, R. D.; Bier, M. *Phys. Rev. Lett.* **1994**, *72*, 1766–1769.
- (29) Prost, J.; Chauwin, J.-P.; Ajdari, A. *Phys. Rev. Lett.* **1994**, *72*, 2652–2655.
- (30) Healy, K.; Siwy, Z.; Morrison, A. P.; Neumann, R. *Biophys. J.*, **2004**, *86*, 552A.
- (31) Heins, E. A.; Baker, L. A.; Siwy, Z.; Mota, M. O.; Martin, C. R. *J. Phys. Chem.* **2005**, *109*, 18400–18407.

NL0524290